Mechanics of Advanced Composite Structures 7 (2020) 355 – 369

Mechanics of Advanced Composite Structures

Semnan University

journal homepage: http://MACS.journals.semnan.ac.ir

Active control of free and forced vibration of rotating laminated composite cylindrical shells embedded with magnetostrictive layers based on classical shell theory

S. Mohammadrezazadeh *, **A. A. Jafari**

Faculty of Mechanical Engineering, K. N. Toosi University of Technology, Tehran, 1991943344, Iran

KEYWORDS

Active vibration control
Classical shell theory
Modified Galerkin method
Magnetostrictive layers
Rotating laminated composite cylindrical shell

ABSTRACT

In this study, active control of free and forced vibration of rotating thin laminated composite cylindrical shells embedded with two magnetostrictive layers is investigated by means of classical shell theory. The shell is subjected to harmonic load exerted to inner surface of the shell in thickness direction. The velocity feedback control method is used in order to obtain the control law. The vibration equations of the rotating cylindrical shell are extracted by means of Hamilton principle while the effects of initial hoop tension, centrifugal and Coriolis accelerations are considered. The partial differential equations of the rotating cylindrical shell are converted to ordinary differential equations by means of modified Galerkin method. The displacement of the shell is obtained using modal analysis. The free vibration results of this study are validated by comparison with the results of published literature. Also, the forced vibration result is compared with the result of fourth order Runge-Kutta method to prove its correctness. Finally, the effects of several parameters including circumferential wave number, rotational velocity, the whole thickness of orthotropic layers, the whole thickness of orthotropic layers, length, the amplitude and exciting frequency of the load on the vibration characteristics of the rotating cylindrical shell are investigated.

1. Introduction

Rotating shells have numerous applications in industry and science fields such as aviation, chemical, aero-space, civil and mechanics [1]. Mechanical behavior of structures has been studied by several researchers. Chen et al. [2] have extracted the general equations for the vibration of high-speed rotating shells of revolution considering the effects of Coriolis acceleration and large deformation. As an example, the vibration responses of rotating cylindrical shells have been derived by the finite element method. Hua and Lam [3] have used Love type shell theory and the generalized differential quadrature method to investigate the influences of boundary conditions on the frequency characteristics of a thin rotating cylindrical shell. Guo et al. [4] have extracted the vibration responses of rotating cylindrical shells by employing finite element method. Zhao et al. [5] have studied the vibration of simply supported rotating cross-ply laminated cylindrical shells with stringers and rings using an energy method. Liew et al. [6] have presented the harmonic reproducing kernel particle method in order to study the free vibration of rotating cylindrical shells. Xu [7] has used three methods for analyzing the forced vibration of an infinite cylindrical shell filled with fluid. Kim and Bolton [8] have investigated the vibration of an inflated rotating circular cylindrical shell in order to understand the effects of rotation on wave propagation within a treadband of a tire. Jafari and Bagheri [9] have used Ritz method and Sander's theorem in order to analyze the free vibration of simply supported rotating cylindrical shells containing circumferential stiffeners. Lee and Han [10] have obtained forced vibration responses of shells and plates under arbitrary loading as well as natural frequencies of composite and isotropic laminates. Li et al. [11] have used Rayleigh-Ritz method in order to investigate forced vibration of conical shells.

* Corresponding author. Tel.: +98-21-84063215; Fax: +98-21-88674748
E-mail address: sh.mrezazadeh@gmail.com

DOI: 10.22075/MACS.2020.16921.1191
Received 2019-01-06; Received in revised form 2019-11-14; Accepted 2020-06-19

Civalek and Gurses [12] have utilized the Love's first approximation shell theory and discrete singular convolution method to analyze free vibration of rotating cylindrical shells. Akgoz and Civalek [13] have studied nonlinear free vibration of thin laminated plates on nonlinear elastic foundations through discrete singular convolution method. Sun et al. [14] have utilized Sanders' shell equations and Fourier series expansion method to present the vibration responses of thin rotating cylindrical shells under various boundary conditions. Ghorbanpour Arani et al. [15] have studied axial buckling of double-walled Boron Nitride nanotubes surrounded by an elastic medium. Barzoki et al. [16] have studied nonlinear buckling of a cylindrical shell on an elastic foundation via harmonic differential quadrature method. Sun et al. [17] have extended a wave propagation approach to investigate the frequency characteristics of thin rotating cylindrical shells. Daneshjou and Talebitooti [18] have accomplished the free vibration study of thick rotating stiffened composite cylindrical shells under different boundary conditions by using a three-dimensional theory. Civalek [19] has obtained nonlinear static and dynamic responses for shallow spherical shells on elastic foundations. Thai and Kim [20] have reviewed various theories used for analysis and modeling of functionally graded plates and shells. Mercan et al. [21] have studied free vibration of functionally graded cylindrical shells using discrete singular convolution method. Civalek [22] has presented free vibration responses for conical and cylindrical shells and annular plates from composite laminated and functionally graded materials. Zhang et al. [23] have presented the free and forced vibration responses of submerged finite elliptic cylindrical shells. Civalek [24] has applied the discrete singular convolution method to study the free vibration of rotating shells. Hussain et al. [25] have derived vibration responses of rotating functionally graded cylindrical shell resting on elastic foundations.

Reviewing literature reveals that improving the rotating circular cylindrical shells behaviour by the active control of their free and forced vibration should be taken into consideration. In this way, the use of smart materials which could be used for active vibration control will be appropriate. Magnetostrictive materials are among smart materials which can be used for active vibration control. Terfenol-D is a magnetostrictive material with high energy density, high relatively available displacements which has wide bandwidth [26]. Several researchers have used magnetostrictive smart materials in order to suppress the vibration of beams [27-29], curved beams [30], plates [31-33] and shells [34-38].

There are several theories for modelling of the shells including classical and first order shear deformation theories. In the classical theory which is used for thin shells, the normal to the mid-surface stays straight and normal to it after deformation [39]; while in first order shear deformation theory, the normal to the middle surface is straight after deformation but it is not normal [40]. The classical theory is simpler and leads to vibration responses with fewer mathematical effort. Therefore, for thin shells the use of classical theory is appropriate. Thus, in this paper classical shell theory is used to study active control of free and forced vibration of rotating laminated composite thin cylindrical shells by means of velocity feedback control law through smart magnetostrictive layers. The shell is under harmonic load which is applied to the inner surface of the shell in thickness direction. The partial differential vibration equations of the rotating laminated composite cylindrical shell are extracted considering the effects of centrifugal and Coriolis forces as well as initial hoop tension. The modified Galerkin method is applied for converting the partial differential equations to ordinary differential equations. The displacement results of the shell are obtained via modal analysis. The accuracy of this study's results is investigated by comparison with the results published in literature for free vibration and with the result of fourth order Runge-Kutta method for forced vibration. The effects of several parameters such as circumferential wave number, rotation speed, the thickness of orthotropic layers, the thickness of each magnetostrictive layer, the length, the amplitude and exciting frequency of the load on the vibration characteristics of the rotating cylindrical shell are investigated.

2. Problem Formulation

2.1. Basic relations

The considered coordinate system (x, θ, z) and geometric characteristics of the rotating thin laminated composite circular cylindrical shell are shown in Fig. 1. The cylindrical shell is composed of 4 layers of glass-epoxy (Gl-Ep) orthotropic material and two magnetostrictive layers used for active vibration control. The schematic of the cylindrical shell layers is shown in Fig. 2. For the rotating cylindrical shell, h_T is the total thickness, h is the thickness of each orthotropic layer, h_m is the thickness of each magnetostrictive layer and h_o is the thickness of whole orthotropic layers. In addition, L is the length, R is the radius and Ω is the constant rotation speed. The longitudinal, circumferential and normal directions of the shell are demonstrated as x, θ and z, respectively. The origin of the coordinate system is located on the middle surface of an arbitrary edge of the shell.

The displacements of a point in the middle surface of the shell in x, θ and z directions are expressed by u_0, v_0 and w_0, respectively. According to classical shell theory, the relations between the displacements of an arbitrary point and displacements of a point in the middle surface of the shell are in the following form [39]:

$$\begin{aligned} u &= u_0 - z\frac{\partial w_0}{\partial x} \\ v &= v_0 + z\left(-\frac{1}{R}\frac{\partial w_0}{\partial \theta} + \frac{v_0}{R}\right) \\ w &= w_0 \end{aligned} \tag{1}$$

while u, v and w demonstrate the displacements of an arbitrary point of the shell in x, θ and z directions, respectively. The relation of strains ($\varepsilon_x, \varepsilon_\theta, \varepsilon_{x\theta}$) with middle surface strains ($\varepsilon_{0x}, \varepsilon_{0\theta}, \varepsilon_{0x\theta}$) and curvature changes ($k_x, k_\theta, k_{x\theta}$) of the rotating cylindrical shell are as follows [39]:

$$\begin{aligned} \varepsilon_x &= \varepsilon_{0x} + zk_x \\ \varepsilon_\theta &= \varepsilon_{0\theta} + zk_\theta \\ \varepsilon_{x\theta} &= \varepsilon_{0x\theta} + zk_{x\theta} \end{aligned} \tag{2}$$

while [39]:

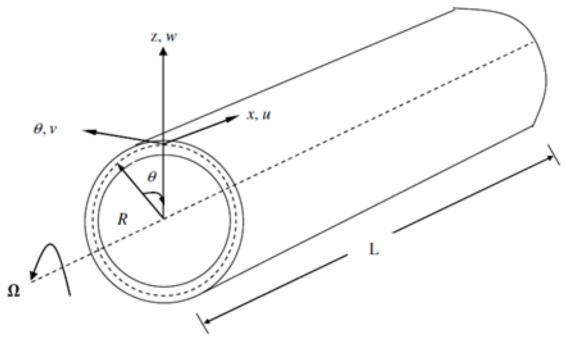

Fig. 1. The coordinate system and geometric characteristics of rotating circular cylindrical shell [12]

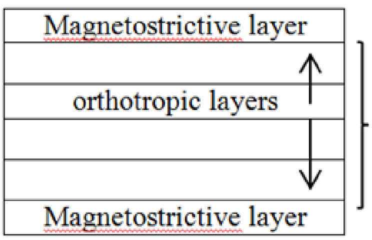

Fig. 2. The schematic of the layers of the considered cylindrical shell

$$\begin{aligned} &\varepsilon_{0x} = \frac{\partial u_0}{\partial x}, \quad \varepsilon_{0\theta} = \frac{1}{R}\frac{\partial v_0}{\partial \theta} + \frac{w_0}{R}, \\ &\varepsilon_{0x\theta} = \frac{\partial v_0}{\partial x} + \frac{1}{R}\frac{\partial u_0}{\partial \theta}, \quad k_x = -\frac{\partial^2 w_0}{\partial x^2} \\ &k_\theta = -\frac{1}{R^2}\frac{\partial^2 w_0}{\partial \theta^2} + \frac{1}{R^2}\frac{\partial v_0}{\partial \theta} \\ &k_{x\theta} = -\frac{2}{R}\frac{\partial^2 w_0}{\partial x \partial \theta} + \frac{1}{R}\frac{\partial v_0}{\partial x} \end{aligned} \tag{3}$$

The relations between the stresses and strains of each layer of the shell (orthotropic layer or magnetostrictive layer) are extracted by the following equation [37]:

$$\begin{Bmatrix} \sigma_x \\ \sigma_\theta \\ \sigma_{x\theta} \end{Bmatrix}^{(k)} = \begin{bmatrix} \bar{Q}_{11} & \bar{Q}_{12} & \bar{Q}_{16} \\ \bar{Q}_{12} & \bar{Q}_{22} & \bar{Q}_{26} \\ \bar{Q}_{16} & \bar{Q}_{26} & \bar{Q}_{66} \end{bmatrix}^{(k)} \begin{Bmatrix} \varepsilon_x \\ \varepsilon_\theta \\ \varepsilon_{x\theta} \end{Bmatrix} - \begin{Bmatrix} \bar{e}_{31} \\ \bar{e}_{32} \\ \bar{e}_{36} \end{Bmatrix}^{(k)} H \tag{4}$$

It should be mentioned that the second part of Eq. (4) which is related to magnetic field H is used only for magnetostrictive layers and is zero for the layers from Gl-Ep material. In addition, in Eq. (4) superscript k is referred to the number of layers and $\bar{Q}_{ij}$ is used to denote transformed stiffness coefficients defined as follows [41]:

$$\begin{aligned} \bar{Q}_{11} &= Q_{11}\cos^4\varphi + 2(Q_{12} + 2Q_{66})\sin^2\varphi\cos^2\varphi \\ &+ Q_{22}\sin^4\varphi \\ \bar{Q}_{12} &= (Q_{11} + Q_{22} - 4Q_{66})\sin^2\varphi\cos^2\varphi \\ &+ Q_{12}(\sin^4\varphi + \cos^4\varphi) \\ \bar{Q}_{22} &= Q_{11}\sin^4\varphi + 2(Q_{12} + 2Q_{66})\sin^2\varphi\cos^2\varphi \\ &+ Q_{22}\cos^4\varphi \\ \bar{Q}_{16} &= (Q_{11} - Q_{12} - 2Q_{66})\sin\varphi\cos^3\varphi \\ &+ (Q_{12} - Q_{22} + 2Q_{66})\sin^3\varphi\cos\varphi \\ \bar{Q}_{26} &= (Q_{11} - Q_{12} - 2Q_{66})\sin^3\varphi\cos\varphi \\ &+ (Q_{12} - Q_{22} + 2Q_{66})\sin\varphi\cos^3\varphi \\ \bar{Q}_{66} &= (Q_{11} + Q_{22} - 2Q_{12} - 2Q_{66})\sin^2\varphi\cos^2\varphi \\ &+ Q_{66}(\sin^4\varphi + \cos^4\varphi) \end{aligned} \tag{5}$$

while φ and Q_{ij} are respectively the angle of each layer with x axis and also the stress-reduced stiffness defined by the following equation [41]:

$$\begin{aligned} &Q_{11} = \frac{E_1}{1 - \nu_{12}\nu_{21}}, \quad Q_{12} = \frac{\nu_{12}E_2}{1 - \nu_{12}\nu_{21}} \\ &Q_{22} = \frac{E_2}{1 - \nu_{12}\nu_{21}}, \quad Q_{66} = G_{12} \end{aligned} \tag{6}$$

The variables E_1, E_2, G_{12} and υ_{12} denote Young's moduli in x and θ directions, shear moduli in the x-θ surface and Poisson's ratio, respectively. The variable H is the magnetic field which is induced by the coil current I as [36, 37]:

$$H = k_c I, \qquad k_c = \frac{n_c}{\sqrt{b_c^2 + 4r_c^2}} \tag{7}$$

The variables k_c, n_c, b_c and r_c introduce magnetic coil constant, the number of the coil turns, coil width and coil radius, respectively. In order to obtain a control law, coil current is introduced as follows:

$$I = \mathrm{C}\left(\dot{w}_0 + \dot{u}_0\right) \tag{8}$$

The coefficient C is a designing parameter which is considered constant in this study. It should be mentioned that the control gain ckc is obtained by multiplying C by k_c. It should be noted that for vibration control, it is necessary to apply the bias point's magnetic field H_b to the system; therefore the whole magnetic field value is: $H_t = H + H_b$. Bias point is the middle point of the linear region of the induced strain versus magnetic field curve of the magnetostricive material [42]. Fig. 3 depicts the schematic diagram of the active vibration mechanism Dused in this paper.

2.2. Hamilton principle

The Hamilton principle [39] is written in the following type for the considered problem:

$$\delta\int_{t_1}^{t_2} \Pi dt = \delta\int_{t_1}^{t_2} \left(T_s - U_h - U_\varepsilon + W\right)dt = 0 \tag{9}$$

while the variables T , U_ε, U_h [43] and W express kinetic energy, strain energy, the work done through centrifugal force and the work done on the shell through external load, respectively. These variables are found via following relations:

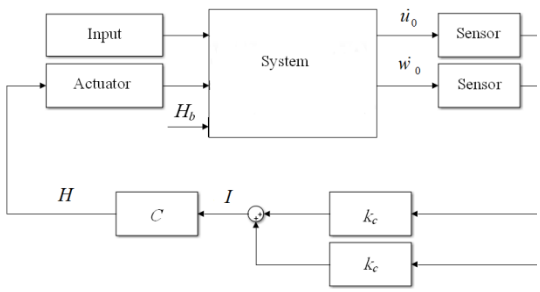

Fig. 3. The schematic diagram for the active vibration control of the rotating cylindrical shell

$$T = \frac{I_1}{2}\int_\theta\int_x \begin{Bmatrix} \left(\dot{u}^2 + \dot{v}^2 + \dot{w}^2\right) \\ +\Omega^2\left(v^2 + w^2\right) \\ +2\Omega\left(\dot{v}w - \dot{w}v\right) \end{Bmatrix} R dx d\theta \tag{10}$$

$$U_\varepsilon = 0.5\sum_{k=1}^{N}\int_\theta\int_x \begin{pmatrix} \sigma_x^{(k)}\varepsilon_x + \sigma_\theta^{(k)}\varepsilon_\theta \\ +\sigma_{x\theta}^{(k)}\varepsilon_{x\theta} \end{pmatrix} R dx d\theta \tag{11}$$

$$\delta U_h = \int_\theta\int_x \frac{N_\theta^0}{R^2} \begin{pmatrix} (R\dfrac{\partial w_0}{\partial x} - \dfrac{\partial^2 u_0}{\partial \theta^2})\delta u_0 \\ -R\dfrac{\partial^2 u_0}{\partial x \partial \theta}\delta v_0 \\ +(\dfrac{\partial v_0}{\partial \theta} - \dfrac{\partial^2 w_0}{\partial \theta^2})\delta w_0 \end{pmatrix} R dx d\theta \tag{12}$$

$$\delta W = \int_\theta\int_x F(x,\theta,t) R \delta \mathrm{w}\, dx d\theta dt \tag{13}$$

while I_1, N_θ^0 and $F(x,\theta,t)$ respectively denote moment of inertia, initial hoop tension [44] and the external load which are defined as:

$$I_1 = \sum_{k=1}^{N}\int_{z_k}^{z_{k+1}} \rho^{(k)} dz \tag{14}$$

$$N_\theta^0 = I_1 \Omega^2 R^2 \tag{15}$$

$$F(x,\theta,t) = f\cos 3\theta \cos\Omega_f t \tag{16}$$

while f and Ω_f denote the amplitude and excitation frequency of the exernal load, respectively.

2.3. Basic vibration equations

Substituting Eqs. (10) to (13) into Eq. (9) leads to the vibration equations of the rotating cylindrical shell in the following form:

$$\begin{aligned} &R\frac{\partial N_x}{\partial x} + \frac{R}{2}\frac{\partial (A_{31}H)}{\partial x} + \frac{\partial N_{x\theta}}{\partial \theta} \\ &+\frac{1}{2}\frac{\partial (A_{36}H)}{\partial \theta} + \frac{N_\theta^0}{R}(-R\frac{\partial w_0}{\partial x} + \frac{\partial^2 u_0}{\partial \theta^2}) \\ &-I_1 R\ddot{u} = 0 \end{aligned} \tag{17}$$

$$\begin{aligned} &\frac{\partial N_\theta}{\partial \theta} + \frac{1}{2}\frac{\partial (A_{32}H)}{\partial \theta} + R\frac{\partial N_{x\theta}}{\partial x} + \frac{R}{2}\frac{\partial (A_{36}H)}{\partial x} \\ &+\frac{1}{R}\frac{\partial M_\theta}{\partial \theta} + \frac{1}{2R}\frac{\partial (B_{32}H)}{\partial \theta} + \frac{\partial M_{x\theta}}{\partial x} \\ &+\frac{1}{2}\frac{\partial (B_{36}H)}{\partial x} + N_\theta^0\frac{\partial^2 u_0}{\partial x \partial \theta} \\ &+I_1 R(-\ddot{v} + \Omega^2 v - 2\Omega\dot{w}) = 0 \end{aligned} \tag{18}$$

$$
\begin{aligned}
&-N_\theta - \frac{A_{32}H}{2} + R\frac{\partial^2 M_x}{\partial x^2} + \frac{R}{2}\frac{\partial^2 (B_{31}H)}{\partial x^2} + \frac{1}{R}\frac{\partial^2 M_\theta}{\partial \theta^2} \\
&+\frac{1}{2R}\frac{\partial^2 (B_{32}H)}{\partial \theta^2} + 2\frac{\partial^2 M_{x\theta}}{\partial x\,\partial \theta} + \frac{\partial^2 (B_{36}H)}{\partial x\,\partial \theta} \\
&+\frac{N_\theta^0}{R}\left(-\frac{\partial v_0}{\partial \theta} + \frac{\partial^2 w_0}{\partial \theta^2}\right) \\
&+I_1 R(-\ddot{w} + \Omega^2 w + 2\Omega \dot{v}) = 0
\end{aligned} \tag{19}
$$

while ($N_x, N_\theta, N_{x\theta}$) and ($M_x, M_\theta, M_{x\theta}$) are in-plane forces and moments obtained in the following type [36]:

$$
\begin{Bmatrix} N_x \\ N_\theta \\ N_{x\theta} \\ M_x \\ M_\theta \\ M_{x\theta} \end{Bmatrix} = \begin{bmatrix} A_{11} & A_{12} & A_{16} & B_{11} & B_{12} & B_{16} \\ A_{12} & A_{22} & A_{26} & B_{12} & B_{22} & B_{26} \\ A_{16} & A_{26} & A_{66} & B_{16} & B_{26} & B_{66} \\ B_{11} & B_{12} & B_{16} & D_{11} & D_{12} & D_{16} \\ B_{12} & B_{22} & B_{26} & D_{12} & D_{22} & D_{26} \\ B_{16} & B_{26} & B_{66} & D_{16} & D_{26} & D_{66} \end{bmatrix} \begin{Bmatrix} \varepsilon_{0x} \\ \varepsilon_{0\theta} \\ \varepsilon_{0x\theta} \\ k_x \\ k_\theta \\ k_{x\theta} \end{Bmatrix} - \begin{Bmatrix} A_{31} \\ A_{32} \\ A_{36} \\ B_{31} \\ B_{32} \\ B_{36} \end{Bmatrix} H \tag{20}
$$

while [36]:

$$
\begin{aligned}
A_{ij} &= \sum_{k=1}^{N} Q_{ij}^{(k)} (z_{k+1} - z_k) \qquad i,j = 1,2,6 \\
B_{ij} &= \frac{1}{2}\sum_{k=1}^{N} Q_{ij}^{(k)} (z_{k+1}^2 - z_k^2) \qquad i,j = 1,2,6 \\
D_{ij} &= \frac{1}{3}\sum_{k=1}^{N} Q_{ij}^{(k)} (z_{k+1}^3 - z_k^3) \qquad i,j = 1,2,6
\end{aligned} \tag{21}
$$

$$
\begin{Bmatrix} A_{31} \\ A_{32} \\ A_{36} \\ B_{31} \\ B_{32} \\ B_{36} \end{Bmatrix} = \sum_{k=m_1,m_2,\ldots}^{N} \int_{z_k}^{z_{k+1}} \begin{Bmatrix} \bar{e}_{31} \\ \bar{e}_{32} \\ \bar{e}_{36} \\ z\bar{e}_{31} \\ z\bar{e}_{32} \\ z\bar{e}_{36} \end{Bmatrix} dz \tag{22}
$$

while $m_1, m_2, \ldots$ express layer numbers of the magnetostrictive layers. Substituting Eqs. (3), (7), (8) and (20) into Eqs. (17) to (19) leads to the following expression:

$$
\begin{bmatrix} L_{11} & L_{12} & L_{13} \\ L_{21} & L_{22} & L_{23} \\ L_{31} & L_{32} & L_{33} \end{bmatrix} \begin{Bmatrix} u_0 \\ v_0 \\ w_0 \end{Bmatrix} = \begin{Bmatrix} 0 \\ 0 \\ -\mathrm{R}F(x,\theta,t) \end{Bmatrix} \tag{23}
$$

while L_{ij} refers to differential operators which are introduced for symmetric cross-ply rotating cylindrical shells in the appendix. In addition, for the rotating cylindrical shells with simply supported boundary conditions, simplification of the Hamilton principle leads to the geometric and natural boundary conditions which are respectively in the forms of Eqs. (24) and (25):

$$
\begin{aligned}
&\delta w_0(0,\theta,t) = 0, \qquad \delta v_0(0,\theta,t) = 0 \\
&\delta w_0(L,\theta,t) = 0, \qquad \delta v_0(\mathrm{L},\theta,t) = 0
\end{aligned} \tag{24}
$$

$$
\begin{aligned}
&-N_x R\delta u_0(0,\theta,t) = 0, M_x R\frac{\partial \delta w_0}{\partial x}(0,\theta,t) = 0 \\
&-N_x R\delta u_0(L,\theta,t) = 0, M_x R\frac{\partial \delta w_0}{\partial x}(L,\theta,t) = 0
\end{aligned} \tag{25}
$$

Natural boundary conditions can be rewritten as following:

$$
[\mathbf{P_{ij}}]\begin{Bmatrix} \mathbf{u_0}(0,\theta) \\ \mathbf{v_0}(0,\theta) \\ \mathbf{w_0}(0,\theta) \end{Bmatrix} = \mathbf{0}, \qquad [\mathbf{P_{ij}}]\begin{Bmatrix} \mathbf{u_0}(L,\theta) \\ \mathbf{v_0}(L,\theta) \\ \mathbf{w_0}(L,\theta) \end{Bmatrix} = \mathbf{0} \tag{26}
$$

while differential operators $\mathbf{P_{ij}}$ are defined in the appendix.

3. Problem solution

Galerkin method is from weighted resudial methods while its solution is considered to be series of comparison functions which satisfy all of the problem's boundary conditions [39]. In this paper, comparison of the Galerkin merthod with Hamilton principle leads to a modified galerkin method which contains natural boundary conditions and is written as following:

$$
\begin{aligned}
&\int_0^L \int_0^{2\pi} \left(\left(\left[\mathbf{L_{ij}} \right] \{\phi\} \{\mathbf{x}\}^T \right) \right) \{\phi\} d\theta dx \\
&+\int_0^{2\pi} \left(\left[\mathbf{P_{ij}} \right] \{\phi\} \{\mathbf{x}\}^T \right) \{\phi\} \Big|_0^L d\theta = \{\mathbf{0}\}
\end{aligned} \tag{27}
$$

The approximayte solution of the considered modified galerkin method is only necessary to satisfy geometric boundary conditions. The following approximate function satisfies geometric boundary conditions of the problem [45]:

$$
\{\phi\} = \begin{Bmatrix} \mathbf{u_0} \\ \mathbf{v_0} \\ \mathbf{w_0} \end{Bmatrix} = \begin{Bmatrix} \sum_{m=1}^{M_T} \sum_{n=0}^{N_T} \cos(\frac{m\pi x}{l}) \{\cos n\theta \mathbf{u_{t1}}(t) - \sin n\theta \mathbf{u_{t2}}(t)\} \\ \sum_{m=1}^{M_T} \sum_{n=0}^{N_T} \sin(\frac{m\pi x}{l}) \{\sin n\theta \mathbf{v_{t1}}(t) + \cos n\theta \mathbf{v_{t2}}(t)\} \\ \sum_{m=1}^{M_T} \sum_{n=0}^{N_T} \sin(\frac{m\pi x}{l}) \{\cos n\theta \mathbf{w_{t1}}(t) - \sin n\theta \mathbf{w_{t2}}(t)\} \end{Bmatrix} \tag{28}
$$

while the variables m and n are respectively introduced longitudinal and circumferential wave numbers. Substituting Eq. (28) into Eq. (27), leads to the following ordinary differential equation for the shell:

$$\begin{gathered}[\mathbf{M}]\{\ddot{\mathbf{x}}\}+([\mathbf{C}]+[\mathbf{C_r}])\{\dot{\mathbf{x}}\}+[\mathbf{K}]\{\mathbf{x}\}=\{\mathbf{f_t}(t)\} \\ \{\mathbf{x}\}=\{\mathbf{u_{t1}},\mathbf{u_{t2}},\mathbf{v_{t1}},\mathbf{v_{t2}},\mathbf{w_{t1}},\mathbf{w_{t2}}\}^T\end{gathered} \tag{29}$$

While $[\mathbf{M}]$, $[\mathbf{K}]$, $[\mathbf{C}]$ and $[\mathbf{C_r}]$ are the mass matrix, stiffness matrix and matrices due to velocity feedback control and rotation of the rotating cylindrical shell, respectively. In addition, $\{\mathbf{f_t}(t)\}$ is the load vector which is only related to variable t. Eq. (29) can be written in state space form as follows [39]:

$$\{\dot{\mathbf{y}}\}=[\mathbf{A}]\{\mathbf{y}\}+[\mathbf{R}], \qquad \{\mathbf{y}\}=\{\mathbf{x},\dot{\mathbf{x}}\}^T \tag{30}$$

While [39]

$$[\mathbf{A}]=\begin{bmatrix}[\mathbf{0}] & [\mathbf{I}] \\ -[\mathbf{M}]^{-1}[\mathbf{K}] & -[\mathbf{M}]^{-1}([\mathbf{C}]+[\mathbf{C_r}])\end{bmatrix} \tag{31}$$

$$[\mathbf{R}]=\begin{bmatrix}[0] \\ [\mathbf{M}]^{-1}\{\mathbf{f}_t\}\end{bmatrix} \tag{32}$$

The eigenvalues of matix $[\mathbf{A}]$ are shown with λ_i. For a determined value of circumferential wave number, backward λ_b and forward λ_f waves are defined as:

$$\begin{Bmatrix}\lambda_f \\ \lambda_b\end{Bmatrix}=\begin{cases}-\beta_f \pm \omega_f i \\ -\beta_b \pm \omega_b i\end{cases} \tag{33}$$

while β_f and ω_f respectively represent forward damping coefficient and forward frequency. On the other hand, β_b and ω_b indicate backward damping coefficient and backward frequency, respectively. The observation results demonstrate that the absolute values of backward waves are generally greater than those of forward waves [44]. For a stationary shell ($\Omega=0$ rps), the magnitudes of both backward and forward waves become identical ($\lambda_s=-\beta\pm\omega i$) while β and ω are respectively damping coefficient and frequency for the stationary cylindrical shell.

The modal analysis is used in order to obtain the displacement of the shell against time. In this way, a linear combination of the right eigenvectors can be considered to be the solution for the state space form of the problem:

$$\{\mathbf{y}(t)\}=[\mathbf{Y}]\{\boldsymbol{\eta}(t)\} \tag{34}$$

while $[\mathbf{Y}]$ and $\boldsymbol{\eta}(t)$ respectively refer to the matrix of right eigenvectors and the vector of modal coordinates [39]. Substituting Eq. (34) into Eq. (30) leads to the following relation:

$$[\mathbf{Y}]\{\dot{\boldsymbol{\eta}}\}=[\mathbf{A}][\mathbf{Y}]\{\boldsymbol{\eta}\}+\{\mathbf{R}\} \tag{35}$$

Multiplying the transpose of the matrix of left eigenvectors ($[\mathbf{Z}]^T$) [39] by the Eq. (35), and then normalization of the matricies of right and left eigenvectors ($[\mathbf{Z}]^T[\mathbf{Y}]=[\mathbf{I}]$) lead to the following formulation:

$$\{\dot{\boldsymbol{\eta}}\}=[\boldsymbol{\lambda}]\{\boldsymbol{\eta}\}+\{\mathbf{q}(t)\} \tag{36}$$

in which

$$[\lambda]=[\mathbf{Z}]^T[\mathbf{A}][\mathbf{Y}], \qquad \{\mathbf{q}\}=[\mathbf{Z}]^T\{\mathbf{R}\} \tag{37}$$

Finally, the time response of Eq. (30) can be obtained as follows:

$$\begin{aligned}\{\mathbf{y}\}&=[\mathbf{Y}]\exp([\boldsymbol{\lambda}]t)\{\boldsymbol{\eta_0}\} \\ &+[\mathbf{Y}]\int_0^t \exp([\boldsymbol{\lambda}](t-\tau))\{\mathbf{q}(\tau)\}d\tau\end{aligned} \tag{38}$$

while $\{\boldsymbol{\eta_0}\}$ refers to initial conditions of the shell. Substituting Eq. (38) into Eq. (28) leads to the displacement of the rotating shell in any direction and any point of the shell.

4. Results and Discussions

In this paper, active control of free and forced vibration of rotating laminated composite cylindrical shells embedded with two smart magnetostrictive layers is studied. It should be mentioned that in the whole of this section, the simply supported boundary conditions in both sides of the shell are considered. At first, in order to validate the accuracy of this study, some numerical results are compared with literature. In this way, Table 1 shows the comparison of frequency parameter results $\omega^*=\omega R\sqrt{\rho/E_{22}}$ of the used method with literature for a three layered orthotropic non-rotating cylindrical shell with stacking sequence [0°/90°/0°]and geometric characteristics of $h/R=0.002$ and $L/R=1$. The relevant material properties of each layer of the considered cylindrical shell are as follows:

$$\begin{gathered}E_{22}=7.6\ \text{GPa}, E_{11}/E_{22}=2.5, G_{12}=4.1\ \text{GPa}, \\ \upsilon_{12}=0.26, \rho=1643\ \text{kg/m}^3, \text{m}=1\end{gathered} \tag{39}$$

Table 1 shows good adaptation between the results of the used method with literature. Table 2 demonstrates the results of non-dimensional backward $\omega_b^* = \omega_b R\sqrt{(1-\upsilon^2)\rho/E}$ and forward $\omega_f^* = \omega_f R\sqrt{(1-\upsilon^2)\rho/E}$ frequencies for a rotating cylindrical shell with various non-dimensional rotating speeds $\Omega^* = \Omega R\sqrt{(1-\upsilon^2)\rho/E}$. The values of different parameters of the cylindrical shell are $\upsilon=0.3, \mathrm{h}=R/500$ and $L = 5R$. Table 2 shows good agreement between the results of this study with literature results.

Now, at the rest of the paper, the effects of different parameters on the active control responses of free and forced vibration of the rotating laminated composite cylindrical shell embedded with two magnetosrictive layers are investigated. The orthotropic and smart magnetostrictive layers are respectively from Gl-Ep and Terfenol-D materials while the lamination scheme $[mag/0°/90°]_S$ is considered. The term mag is used to represent magnetostrictive layers. The constants of Gl-Ep and Terfenol-D are tabulated in Table 3.

In addition, the values of the shell properties are: L=0.3 m, R=1 m, h=1 mm, h_m=2 mm, $|ckc|=2\times10^4$, $n=3$, $M_T=3$ and $\Omega=10$ rps unless other values are noted. In addition the forced vibration is induced from a load which acts harmonically to the inner surface of the shell in thickness direction with amplitude and excitation frequency of $f=20$ KPa and $\Omega_f=50$ rad/s unless other values are mentioned. It should be mensioned that all of the diagrams of displacement versus time are obtained in thickness direction for a point on the shell with location $(x,\theta,z)=(0.5L,0,0)$. At first it is necessary to validate the forced vibration responses. For this purpose, Fig. 4 compares the displacement result of modal analysis with the result of the fourth order Runge-Kutta method. This figure shows excellent agreement between the results of these two methods.

Figs. 5(a) and (b) respectively show the diagrams of backward and forward damping coefficients versus the circumferential wave number n for different values of rotation speed Ω. Figs. 5(a) and (b) demonstrate that the increase of circumferential wave number leads to the decrease of both backward and forward damping coefficients. In addition, it can be concluded from Figs. 5 (a) and (b) that for a fixed value of n, rotation speed has negligible effect on the values obtained for backward or forward damping coefficients. Figs. 6(a) and (b) respectively depict the variations of the values of backward and forward frequencies versus n for different values of Ω. Figs. 6 (a) and (b) demonstrate that for a constant Ω, the values of backward and forward frequencies decrease with increase of circumferential wave number. Besides, for a determined value of n in the range of almost $n>6$, the increase of rotation speed leads to the observable increase of the backward and forward frequencies. This may be caused because of the presence of terms $\Omega^2 n^2$ or $\Omega^2 n$ in the stiffness matrix obtained from simplifying the differential operators L_{ij} as illustrated in section 3 of this study.

Table 1. Comparison of the frequency parameter responses of a non-rotating laminated cylindrical shell with literature

n	Present	Ref [44]	Error percent (%)
1	1.061596	1.061284	0.03
2	0.804583	0.804054	0.07
3	0.599444	0.598331	0.19
4	0.452652	0.450144	0.56
5	0.350831	0.345253	1.62
6	0.282504	0.270754	4.34

Table 2. Comparison of non-dimensional backward and forward frequencies with literature for a rotating isotropic cylindrical shell with different rotating speeds

Ω^*	n	Backward			Forward		
		Percent	Ref. [46]	Error percent (%)	Percent	Ref [46]	Error percent (%)
0	1	0.1860	0.1875	0.8	0.1860	0.1875	0.8
	3	0.0382	0.0386	1.04	0.0382	0.0386	1.04
0.03	3	0.1035	0.1036	0.10	0.0673	0.0674	0.15
	1	0.2321	0.2336	0.64	0.1371	0.1385	1.01
0.05	3	0.1630	0.1631	0.06	0.1026	0.1027	0.10
0.1	1	0.2749	0.2765	0.58	0.0853	0.0868	1.73

Table 3. The values of the constants of Gl-Ep and Terfenol-D materials [36]

materal	E_{11} (GPa)	E_{22} (GPa)	G_{12} (GPa)	ν_{12}	ρ (kgm^{-3})
Gl-Ep	53.78	17.93	8.96	0.56	1900
Terfenol-D	26.5	26.5	13.25	0	9250

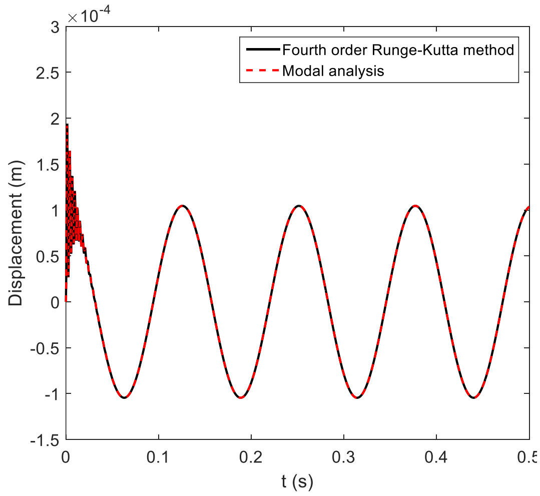

Fig. 4. Comparison of the diagrams of displacement versus time obtained using modal analysis and fourth order Runge-Kutta method.

Figures 7 (a) and (b) respectively show diagrams of backward and forward damping coefficients against the thickness of the whole orthotropic layers h_o for different values of Ω while $h_m = 1$ mm . Figs. 7 (a) and (b) indicate that for a constant value of rotation speed, the values of backward and forward damping coefficients decrease as h_o increases. In addition, for a constant value of h_o , the effect of rotation speed on the values of damping coefficients is negligible. Figs. 8 (a) and (b) respectively depict the curves of backward and forward frequencies against the whole orthotropic layers' thickness h_o for $h_m = 1$ mm . One can conclude from Figs. 8 (a) and (b) that the increase of h_o leads to the increase of both backward and forward frequencies. On the hand, for a constant value of h_o , rotating speed has negligible effect on the backward and forward frequencies.

Figure 9 demonstrates the effect of h_o on the displacement in normal direction which is caused due to the external loading while $h_m = 1$ mm . Fig. 9 shows that the increase of h_o leads to the decrese of the amplitude of the displacement. In addition, this figure shows that using active vibration control leads to effective damping of the noises of the displacement.

Fig. 10 (a) shows the effect of the thickness of each magnetostrictive layer on the curves of backward and forward damping coefficients against rotation speed. One can conclude from Fig. 10 (a) that the increase of the thickness of each magnetostrictive layer leads to greater values for backward and forward frequencies. Fig. 10 (b) depicts the curves of backward and forward frequencies against rotation speed for different values of the thickness of each magnetostrictive layer. It is obvious from this figure that the increase of the thickness of each magnetostrictive layer leads to decrease of both backward and forward frequencies.

Fig. 11 demonstrates the effect of the thickness of each magnetostrictive layer on the displacement in thickness direction caused due to external loading. This figure demonstrates that the increase of the thickness of each magnetostrictive layer leads to the decrees of the vibration amplitude.

Fig. 12(a) shows the variation of backward and forward damping coefficients versus rotation speed for different values of length. This figure demonstrates that for a constant value of rotating speed, backward and forward damping coefficients get larger values as the value of length becomes smaller. In addition, for each value of L , the values of backward and forward damping coefficients respectively increase and decrease with the increase of rotation speed.

a.

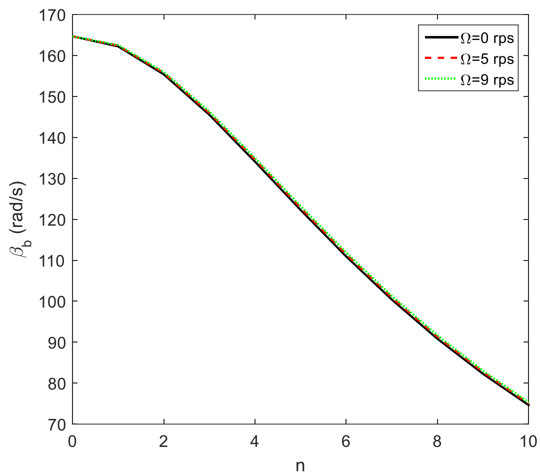

b.

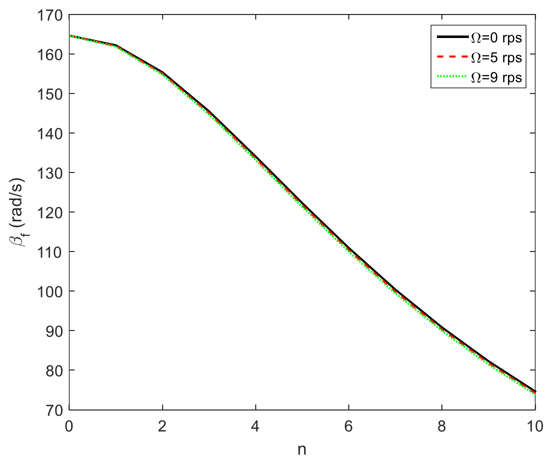

Fig. 5. The variation of backward and forward damping coefficients with circumferential wave number for different values of rotation speed

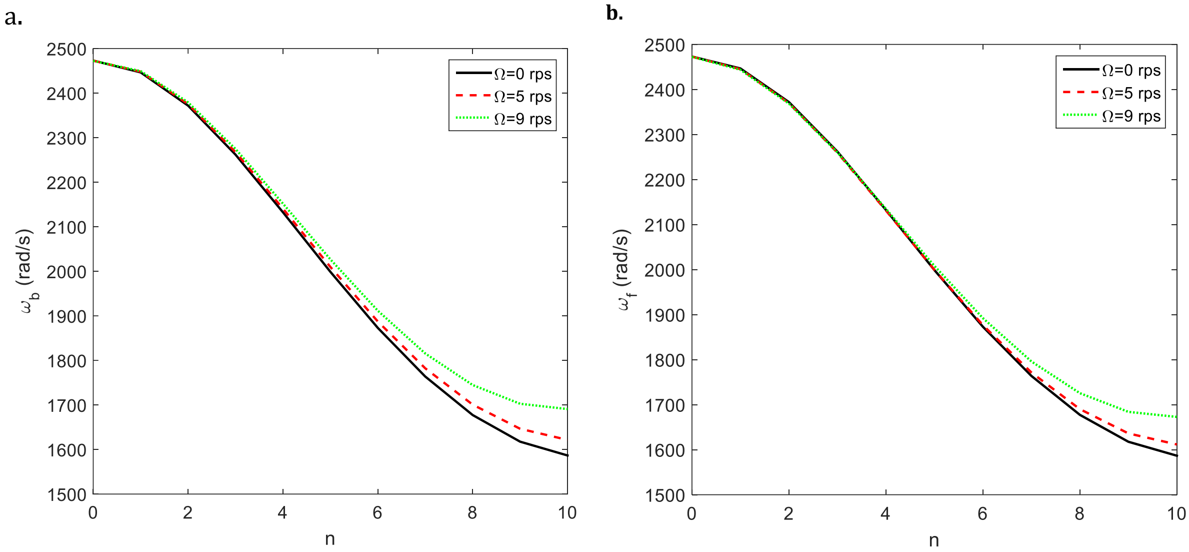

Fig. 6. Diagrams of the backward and forward frequencies versus circumferential wave number for different values of rotational velocity

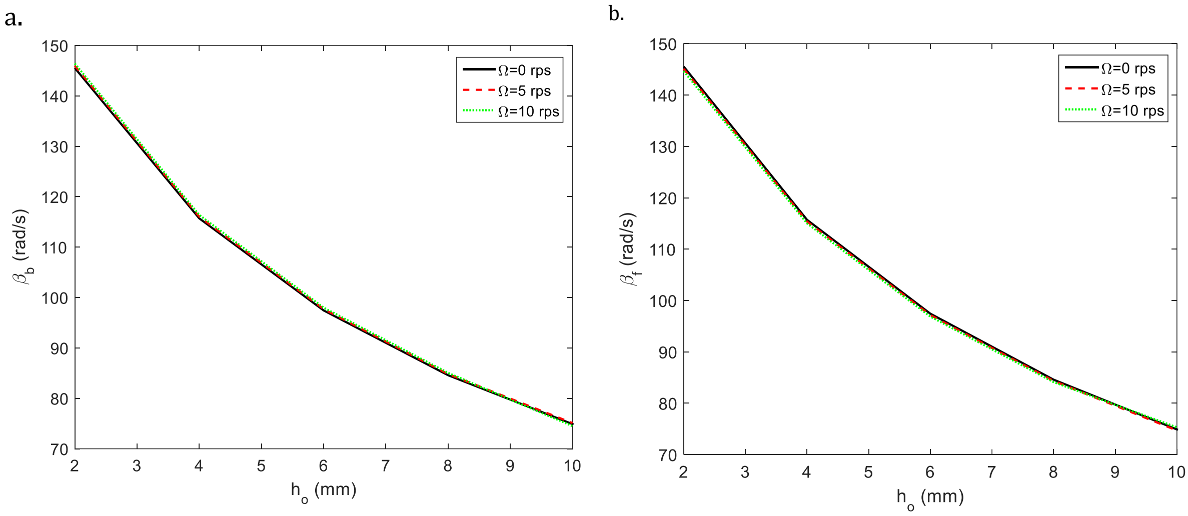

Fig. 7. Diagrams of backward and forward damping coefficients against the whole thickness of orthotropic layers for different rotation speeds

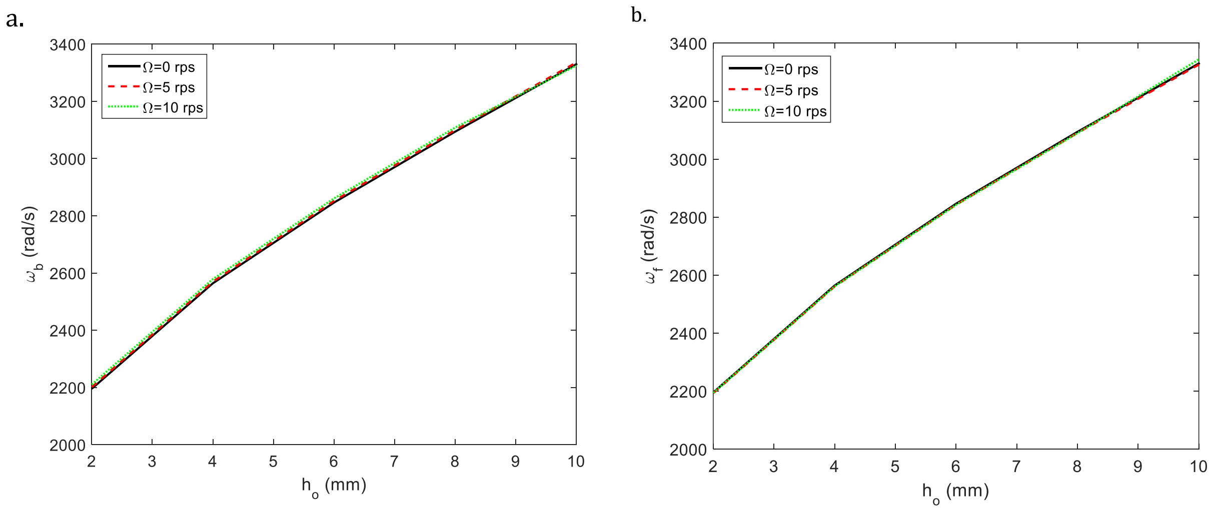

Fig. 8. Diagrams of backward and forward frequencies against the whole thickness of orthotropic layers for different rotational velocities

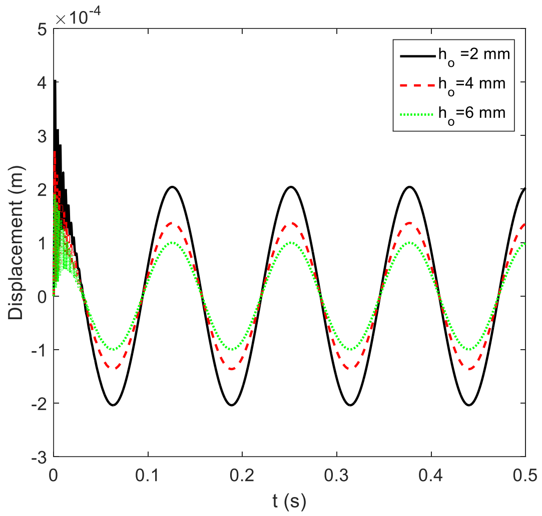

Fig. 9. The influence of the whole thickness of the orthotropic layers on the forced vibration of the shell

Figure 12 (b) depicts the backward and forward frequencies versus rotation speed for different values of length. This figure illustrates that for a constant value of rotation speed, absolute values of backward and forward frequencies become larger as L gets smaller values. In addition, for a constant value of length, the value of backward frequency increases as rotation speed becomes larger.

Figure 13 depicts the influence of the length value on the forced vibration of the shell. This figure shows that the shell with greater value of length has higher amplitude of the displacement.

Fig. 14 shows the diagram of the displacement against time for different values of the rotation speed. This figure shows that increase of the rotation speed has negligible effect on the displacement of the shell due to the external loading.

Fig. 15 depicts diagrams of displacement against time for different values of the amplitude of the external load. It is obvious from Fig. 15 that the increase of the load amplitude leads to the increase of the amplitude of the shell's displacement in thickness direction.

Figs. 16 (a) and (b) demonstrate the diagrams of the displacement against exciting frequency of the external load for non-controlled and controlled shells, respectively. It should be mentioned that the backward and forward frequencies of this uncontrolled shell are obtained as 2281.3314 rad/s and 2265.1189 rad/s, respectively. Fig. 16 (a) depicts that this diagram has peaks approximately in the points that the exciting frequency coincides with the frequencies of the system.

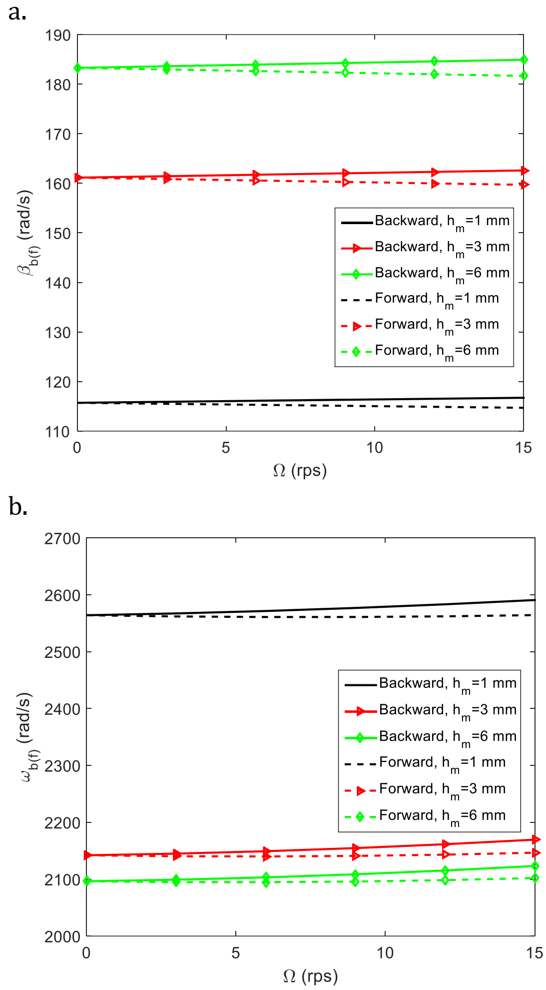

Fig. 10. The influence of "the thickness of each magnetostrictive layer on the curves of forward and backward, a. damping coefficients, b. frequencies, against rotation speed

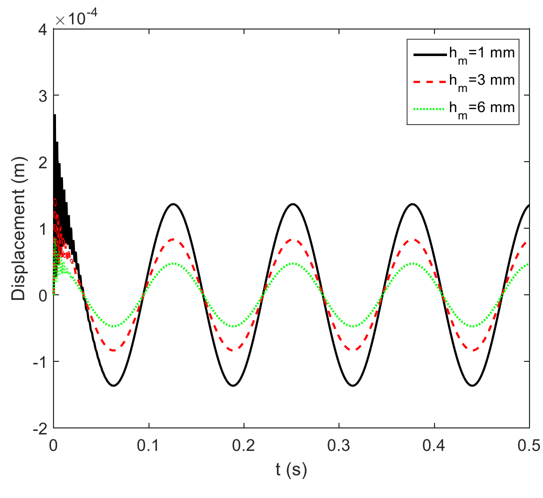

Fig. 11. The effect of the thickness of each magnetostrictive layer on the forced vibration responses of the rotating cylindrical shell

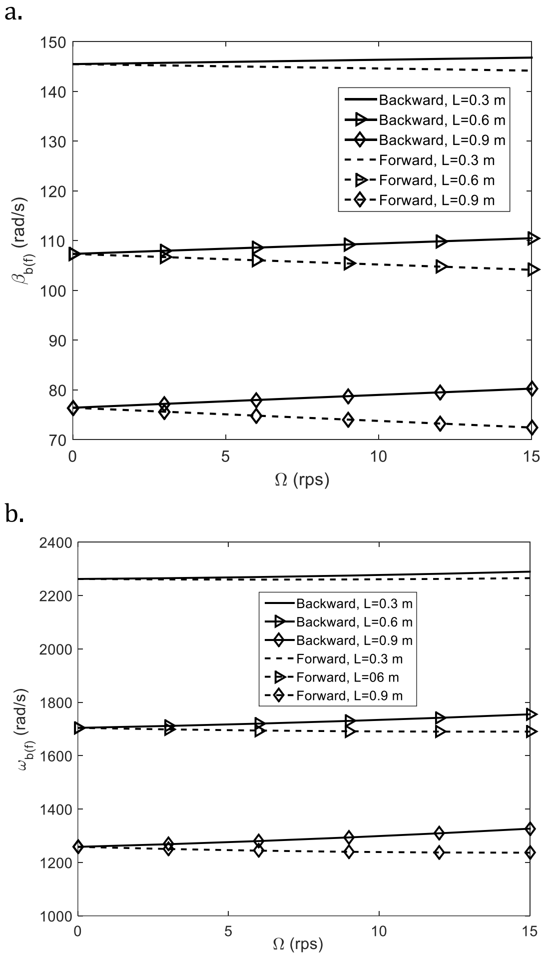

Fig. 12. The variation of backward and forward, a. damping coefficients, b. frequencies, with rotation speed for different values of length

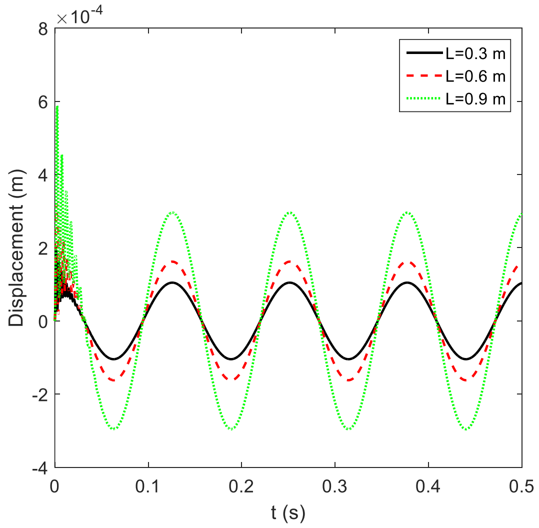

Fig. 13. The effect of the length on the diagrams of the displacement versus time induced through external loading

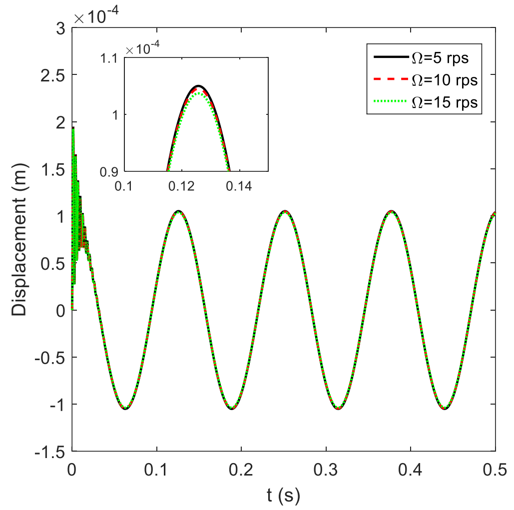

Fig. 14. Diagrams of displacement versus time for different values of rotational velocity

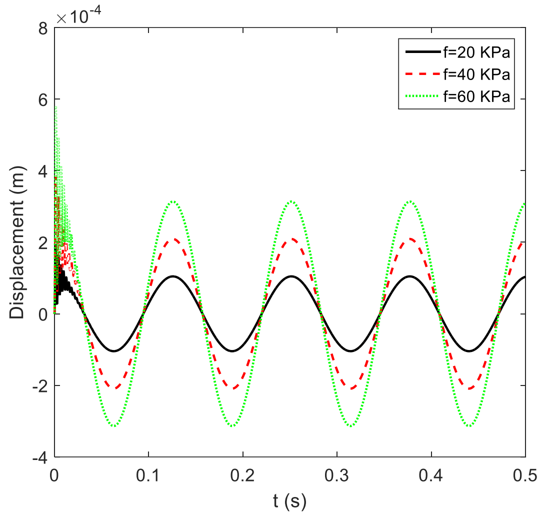

Fig. 15. The effect of the amplitude of the load on the diagram of the displacement versus time

It should be mentioned that resonance phenomenon takes place when the exciting frequency coincides with the natural frequency of the system which leads to dangerous deflections and failure [47]. It is obvious from this figure that displacement in these points is relatively very large which may lead to the failure of the system. Fig. 16 (b) shows that using the designed active vibration control leads to effective decrease of the displacement and the improvement of the shell behavior.

5. Conclusions

In this study, active control of free and forced vibration of thin rotating laminated composite cylindrical shells embedded with two magnetostrictive layers on its outer and inner surfaces is investigated based on classical shell theory. The motion equations of the rotating shell are derived through Hamilton principle considering the effects of Coriolis and centrifugal forces as well as initial hoop tension.

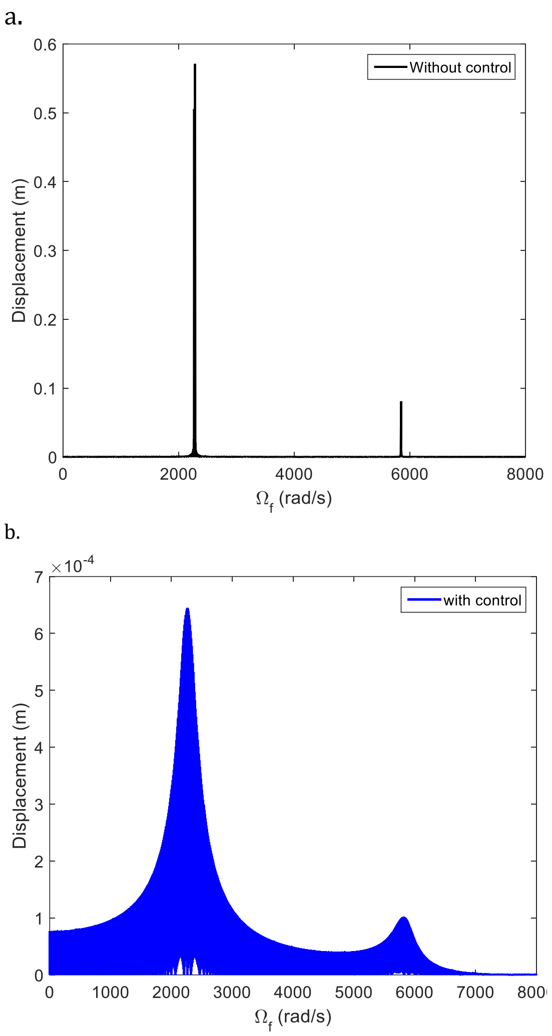

Fig. 16. The effect of the active vibration control on the diagram of the displacement versus exciting frequency

The shell is under external loading which acts harmonically to the inner surface of the shell. The partial differential equations of the shell are converted to ordinary differential equations by means of modified Galerkin method. The displacement response is obtained using modal analysis. The accuracy of the used method for free vibration responses is proved by comparison of some results with the results of non-rotating and rotating cylindrical shells of literature. In addition, the validation of the forced vibration results is obtained by comparison with the result of the fourth order Runge-Kutta method. The effects of circumferential wave number, rotation speed, thickness of the whole orthotropic layers, the thickness of each magnetostrictive layer, length, the amplitude of the load and the exciting frequency of the load on the vibration characteristics of the rotating laminated composite cylindrical shell are investigated.

It can be concluded that the increase of circumferential wave number, the whole orthotropic layers thickness or length leads to the decrease of damping coefficients and increase of the frequencies. On the other hand, the increase of the thickness of each magnetostrictive layer makes greater values for damping coefficients and smaller values for frequencies. The results also show that the increase of "the thickness of each magnetostrictive layer or the whole thickness of the orthotropic layers leads to smaller amplitude for the forced vibration. On the other hand, the value of the forced vibration amplitude increases as the value of the length or the load amplitude increases. In addition, the amplitude of forced vibration has negligible change due to the increase of the rotation speed. Besides, the use of active vibration control leads to the effective decrease of the value of shell displacement in resonance condition.

Appendix

The differential operators L_{ij} for the rotating symmetric cross-ply cylindrical shell used in this study are defined as:

$$L_{11}=-I_1R\frac{\partial^2}{\partial t^2}-\frac{ckcA_{31}R}{2}\frac{\partial^2}{\partial x\,\partial t}+A_{11}R\frac{\partial^2}{\partial x^2}+\frac{A_{66}}{R}\frac{\partial^2}{\partial\theta^2}+A_{11}R\frac{\partial^2}{\partial x^2}+\frac{A_{66}}{R}\frac{\partial^2}{\partial\theta^2}+\frac{N_\theta^{\ 0}}{R}\frac{\partial^2}{\partial\theta^2} \tag{40}$$

$$L_{12}=A_{12}\frac{\partial^2}{\partial x\partial\theta}+A_{66}\frac{\partial^2}{\partial x\partial\theta} \tag{41}$$

$$L_{13}=\frac{-ckcA_{31}R}{2}\frac{\partial^2}{\partial x\,\partial t}+A_{12}\frac{\partial}{\partial x}-N_\theta^{\ 0}\frac{\partial}{\partial x} \tag{42}$$

$$L_{21}=\frac{-ckcA_{32}}{2}\frac{\partial^2}{\partial\theta\partial t}+A_{66}\frac{\partial^2}{\partial x\,\partial\theta}+A_{12}\frac{\partial^2}{\partial x\,\partial\theta}+N_\theta^{\ 0}\frac{\partial^2}{\partial x\,\partial\theta} \tag{43}$$

$$L_{22}=-I_1R\frac{\partial^2}{\partial t^2}+A_{66}R\frac{\partial^2}{\partial x^2}+\frac{A_{22}}{R}\frac{\partial^2}{\partial\theta^2}+\frac{D_{22}}{R^3}\frac{\partial^2}{\partial\theta^2}+\frac{D_{66}}{R}\frac{\partial^2}{\partial x^2}+I_1R\Omega^2 \tag{44}$$

$$L_{23}=-\frac{ckcA_{32}}{2}\frac{\partial^2}{\partial\theta\partial t}+\frac{A_{22}}{R}\frac{\partial}{\partial\theta}-\frac{D_{12}}{R}\frac{\partial^3}{\partial x^2\partial\theta}-\frac{D_{22}}{R^3}\frac{\partial^3}{\partial\theta^3}-\frac{2D_{66}}{R}\frac{\partial^3}{\partial x^2\partial\theta}-2I_1\Omega R\frac{\partial}{\partial t} \tag{45}$$

$$L_{31}=\frac{ckcA_{32}}{2}\frac{\partial}{\partial t}-A_{12}\frac{\partial}{\partial x} \tag{46}$$

$$L_{32}=-\frac{A_{22}}{R}\frac{\partial}{\partial\theta}+\frac{D_{12}}{R}\frac{\partial^3}{\partial x^2\partial\theta}+\frac{D_{22}}{R^3}\frac{\partial^3}{\partial\theta^3}+\frac{2D_{66}}{R}\frac{\partial^3}{\partial x^2\partial\theta}+2RI_1\Omega\frac{\partial}{\partial t}-\frac{N_\theta^{\ 0}}{R}\frac{\partial}{\partial\theta} \tag{47}$$

$$L_{33} = -D_{11}R\frac{\partial^4}{\partial x^4} - \frac{2D_{12}}{R}\frac{\partial^4}{\partial x^2 \partial\theta^2} + \frac{ckcA_{32}}{2}\frac{\partial}{\partial t}$$
$$-\frac{4D_{66}}{R}\frac{\partial^4}{\partial x^2 \partial\theta^2} - \frac{D_{22}}{R^3}\frac{\partial^4}{\partial\theta^4} - \frac{A_{22}}{R} - I_1 R\frac{\partial^2}{\partial t^2} \quad (48)$$
$$+I_1\Omega^2 R + \frac{N_\theta^{\;0}}{R}\frac{\partial^2}{\partial\theta^2}$$

The differential variables P_{ij} are obtained in the following type for the rotating symmetric cross-ply cylindrical shell of this study:

$$P_{11} = \frac{ckcA_{31}R}{2}\frac{\partial}{\partial t} - A_{11}R\frac{\partial}{\partial x} \quad (49)$$

$$P_{12} = -A_{12}\frac{\partial}{\partial\theta} \quad (50)$$

$$P_{13} = \frac{ckcA_{31}R}{2}\frac{\partial}{\partial t} - A_{12} \quad (51)$$

$$P_{32} = \frac{D_{12}}{R}\frac{\partial}{\partial\theta} \quad (52)$$

$$P_{33} = -D_{11}R\frac{\partial^2}{\partial x^2} - \frac{D_{12}}{R}\frac{\partial^2}{\partial\theta^2} \quad (53)$$

$$P_{21} = P_{22} = P_{23} = 0 \quad (54)$$

References

[1] Civalek, O., 2007. A parametric study of the free vibration analysis of rotating laminated cylindrical shells using the method of discrete singular convolution. *Thin-Walled Structures,* 45 (7-8), pp.692-698.

[2] Chen, Y., Zhao, H. B., Shen, Z. P., Grieger I. and Kröplin, B. H., 1993. Vibrations of high speed rotating shells with calculations for cylindrical shells. *Journal of Sound and Vibration*, 160(1), pp.137-160.

[3] Hua, L. I., Lam, K. Y., 1998. Frequency characteristics of a thin rotating cylindrical shell using the generalized differential quadrature method. *International Journal of Mechanical Sciences*, 40(5), pp.443-459.

[4] Guo, D., Chu, F. L., Zheng, Z. C., 2001. The influence of rotation on vibration of a thick cylindrical shell. *Journal of sound and vibration*, 242(3), pp.487-505.

[5] Zhao, X., Liew, K. M., Ng, T. Y., 2002. Vibrations of rotating cross-ply laminated circular cylindrical shells with stringer and ring stiffeners. *International Journal of Solids and Structures*, 39(2), pp.529-545.

[6] Liew, K. M., Ng, T. Y., Zhao, X., Reddy, J. N., 2002. Harmonic reproducing kernel particle method for free vibration analysis of rotating cylindrical shells. *Computer Methods in Applied Mechanics and Engineering*, 191(37-38), pp.4141-4157.

[7] Xu, M. B., 2003. Three methods for analyzing forced vibration of a fluid-filled cylindrical shell. *Applied Acoustics*, 64(7), pp.731-752.

[8] Kim, Y. J., Bolton, J. S., 2004. Effects of rotation on the dynamics of a circular cylindrical shell with application to tire vibration. *Journal of sound and vibration*, 275(3-5), pp.605-621.

[9] Jafari, A. A., 2006. Bagheri M. Free vibration of rotating ring stiffened cylindrical shells with non-uniform stiffener distribution. *Journal of sound and vibration*, 296(1-2), pp.353-367.

[10] Lee, W. H. and Han, S. C., 2006. Free and forced vibration analysis of laminated composite plates and shells using a 9-node assumed strain shell element. *Computational Mechanics*, 39(1), pp.41-58.

[11] Li, F. M., Kishimoto, K., Huang, W. H., 2009. The calculations of natural frequencies and forced vibration responses of conical shell using the Rayleigh–Ritz method. *Mechanics Research Communications*, 36(5), pp.595-602.

[12] Civalek, O., Gürses, M., 2009. Free vibration analysis of rotating cylindrical shells using discrete singular convolution technique. *International Journal of Pressure Vessels and Piping*, 86(10), pp.677-683.

[13] Akgoz, B., Civalek, O., 2011. Nonlinear vibration analysis of laminated plates resting on nonlinear two-parameters elastic foundations. *Steel and Composite Structures*, 11(5), pp.403-421.

[14] Sun, S., Chu, S., Cao, D., 2012. Vibration characteristics of thin rotating cylindrical shells with various boundary conditions. *Journal of Sound and Vibration*, 331(18), pp.4170-4186.

[15] Arani, A. G., Amir, S., Shajari, A. R. and Mozdianfard, M. R., 2012. Electro-thermo-mechanical buckling of DWBNNTs embedded in bundle of CNTs using nonlocal piezoelasticity cylindrical shell theory. *Composites Part B: Engineering*, 43(2), pp.195-203.

[16] Barzoki, A. M., Arani, A. G., Kolahchi, R., Mozdianfard, M. R. and Loghman, A., 2013. Nonlinear buckling response of embedded piezoelectric cylindrical shell reinforced with BNNT under electro–thermo-mechanical loadings using HDQM. Composites Part B: Engineering, 44(1), pp.722-727.

[17] Sun, S., Cao, D., Chu, S., 2013. Free vibration analysis of thin rotating cylindrical shells using wave propagation approach. *Archive of Applied Mechanics*, 83(4), pp.521-531.

[18] Daneshjou, K. and Talebitooti, M., 2014. Free vibration analysis of rotating stiffened composite cylindrical shells by using the layerwise-differential quadrature (LW-DQ) method. *Mechanics of Composite Materials*, 50(1), pp.21-38.

[19] Civalek, Ö., 2014. Geometrically nonlinear dynamic and static analysis of shallow spherical shell resting on two-parameters elastic foundations. *International Journal of Pressure Vessels and Piping*, 113, pp.1-9.

[20] Thai, H. T. and Kim, S. E., 2015. A review of theories for the modeling and analysis of functionally graded plates and shells. *Composite Structures*, 128, pp.70-86.

[21] Mercan, K., Demir, Ç., Civalek, Ö., 2016. Vibration analysis of FG cylindrical shells with power-law index using discrete singular convolution technique. *Curved and Layered Structures*, 3(1), pp.92-90.

[22] Civalek, Ö., 2017. Free vibration of carbon nanotubes reinforced (CNTR) and functionally graded shells and plates based on FSDT via discrete singular convolution method. *Composites Part B: Engineering*, 111, pp.45-59.

[23] Zhang, G. J., Li, T. Y., Zhu, X., Yang, J., Miao, Y. Y., 2017. Free and forced vibration characteristics of submerged finite elliptic cylindrical shell. *Ocean Engineering*, 129, pp.92-106.

[24] Civalek, O., 2017. Discrete singular convolution method for the free vibration analysis of rotating shells with different material properties. *Composite Structures*, 160, pp.267-279.

[25] Hussain, M., Naeem, M. N. and Isvandzibaei, M. R., 2018. Effect of Winkler and Pasternak elastic foundation on the vibration of rotating functionally graded material cylindrical shell. *Proceedings of the Institution of Mechanical Engineers, Part C: Journal of Mechanical Engineering Science*, 232(24), pp.4564-4577.

[26] Goodfriend, M. J. and Shoop, K. M., 1992. Adaptive characteristics of the magnetostrictive alloy, Terfenol-D, for active vibration control. *Journal of intelligent material systems and structures*, 3(2), pp.245–254.

[27] Murty, A. K., Anjanappa, M. and Wu, Y. F., 1997. The use of magnetostrictive particle actuators for vibration attenuation of flexible beams. *Journal of Sound and Vibration*, 206(2), pp.133-149.

[28] Reddy, J. N. and Barbosa, J. I., 2000. On vibration suppression of magnetostrictive beams. *Smart Materials and Structures*, 9(1), p.49.

[29] Kumar, J. S., Ganesan, N., Swarnamani, S. and Padmanabhan, C., 2003. Active control of beam with magnetostrictive layer. *Computers & structures*, 81(13), pp.1375-1382.

[30] Bayat, R., Jafari, A. A. and Rahmani, O., 2015. Analytical solution for free vibration of laminated curved beam with magnetostrictive layers. *International Journal of Applied Mechanics*, 7(03), 1550050.

[31] Kumar, J. S., Ganesan, N., Swarnamani, S. and Padmanabhan, C., 2004. Active control of simply supported plates with a magnetostrictive layer. *Smart materials and structures*, 13(3), p.487.

[32] Zhang, Y., Zhou, H. and Zhou, Y., 2015, Vibration suppression of cantilever laminated composite plate with nonlinear giant magnetostrictive material layers. *Acta Mechanica Solida Sinica*, 28(1), pp.50-61.

[33] Ghorbanpour Arani, A., Khoddami Maraghi, Z. and Khani Arani, H., 2017. Vibration control of magnetostrictive plate under multi-physical loads via trigonometric higher order shear deformation theory. *Journal of Vibration and Control*, 23(19), pp.3057-3070.

[34] Kumar, J. S., Ganesan, N., Swarnamani, S. and Padmanabhan, C., 2003. Active control of cylindrical shell with magnetostrictive layer. *Journal of Sound and vibration*, 262(3), pp.577-589.

[35] Qian, W., Liu, G. R., Chun, L. and Lam, K. Y., 2003. Active vibration control of composite laminated cylindrical shells via surface-bonded magnetostrictive

layers. *Smart materials and structures,* 12(6), p.889.

[36] Pradhan, S. C. and Reddy, J. N., 2004. Vibration control of composite shells using embedded actuating layers. *Smart materials and structures*, 13(5), p.1245.

[37] Lee, S. J. and Reddy, J. N., 2004. Vibration suppression of laminated shell structures investigated using higher order shear deformation theory. *Smart Materials and Structures*, 13(5), p.1176.

[38] Pradhan, S. C., 2005. Vibration suppression of FGM shells using embedded magnetostrictive layers. *International Journal of Solids and Structures*, 42(9-10), pp.2465-2488.

[39] Rao, S. S., 2007. *Vibration of Continuous Systems*. JOHN WILEY & SONS, INC.

[40] Qatu, M. S., 2004. *Vibration of laminated shells and plates*. Elsevier.

[41] Reddy, J. N., 2004. *Mechanics of laminated composite plates and shells: theory and analysis*. CRC Press.

[42] Chopra, I. and Sirohi, J., 2013. *SMART STRUCTURES THEORY*. Cambridge University Press.

[43] Talebitooti, M., 2013. Three-dimensional free vibration analysis of rotating laminated conical shells: layerwise differential quadrature (LW-DQ) method. *Archive of Applied Mechanics*, 83(5), pp.765-781.

[44] Li, H., Lam, K. Y. and Ng, T. Y., 2005. *Rotating shell dynamics*. Elsevier.

[45] Sun, S., Liu, L. and Cao, D., 2018. Nonlinear travelling wave vibrations of a rotating thin cylindrical shell. *Journal of Sound and Vibration*, 431, pp.122-136.

[46] Qinkai, H. and Fulei, C., 2013. Effect of rotation on frequency characteristics of a truncated circular conical shell. *Archive of Applied Mechanics*, 83(12), pp.1789-1800.

[47] Rao, S. S., 2011. *Mechanical vibrations*. Prentice Hall.